Beyond the Lambertian Assumption: A generative model for Apparent BRDF fields of Faces using Anti-Symmetric Tensor Splines*

Angelos Barmpoutis, Ritwik Kumar, Baba C. Vemuri and Arunava Banerjee
Department of Computer and Information Science and Engineering, University of Florida
{abarmpou, rkkumar, vemuri, arunava}@cise.ufl.edu

Abstract

Human faces are neither exactly Lambertian nor entirely convex and hence most models in literature which make the Lambertian assumption, fall short when dealing with specularities and cast shadows. In this paper, we present a novel anti-symmetric tensor spline (a spline for tensor-valued functions) based method for the estimation of the Apparent BRDF (ABRDF) field for human faces that seamlessly accounts for specularities and cast shadows. Furthermore, unlike other methods, it does not require any 3D information to build the model and can work with as few as 9 images. In order to validate the accuracy of our anti-symmetric tensor spline model, we present a novel approximation of the ABRDF using a continuous mixture of single-lobed spherical functions. We demonstrate the effectiveness of our anti-symmetric tensor-spline model in comparison to other popular models in the literature, by presenting extensive results for face relighting and face recognition using the Extended Yale B database.

1. Introduction

BRDF measurements have attracted immense interest from both the vision and graphics community. To measure the BRDF, which is a function of both viewing and illumination directions, two popular methods are prevalent. The first one uses an equipment called the gonioreflectometer where measurements with explicit control over viewing and illumination directions can be made [9]. The second class of techniques use what is called the image based approach, where a single image of the curved surface is used to provide multiple samples of the BRDF in various illumination and viewing directions [20, 18].

Partly due to the inherent efficiency of image based measurements and partly due to the nature of the object in question, BRDF measurements of human faces have largely been done using the image based approach [16, 8]. Depending on the application they target, the methods in the second class can be further categorized into ones which use very specialized and expensive equipment to capture the details of the human face (e.g. Borshukov and Lewis [5] used various specialized equipments and softwares to render faces in the movie "The matrix reloaded", Weyrich *et al*. [24] used custom built devices to measure skin reflectance and sub-surface scattering to render novel face images) and those which work with images from standard face databases like Extended Yale [11, 16] or CMU PIE [21]. The method we propose belongs to this later class of techniques. Using as few as nine images from standard databases, we are able to construct the apparent BRDF (ABRDF) field of the human face, taking into account specularity and cast shadows.

Most of the existing methods, which do not require any specialized equipment for image based BRDF measurements, make the simplifying assumption that the face is a convex Lambertian object [2, 19, 23, 25, 11, 16], which, as we demonstrate (in Fig. 3), is clearly not accurate (as it does not account for specularities and the cast shadows). Even with such a simplifying assumption, some of these techniques end up using 3D information (which is expensive to acquire) [2, 23, 25, 10] and/or require undesirable manual intervention [23, 25]. The existing techniques which do not require explicit 3D information like those proposed in [26, 22], suffer from the usual problems with shape from shading or, as proposed in [13], require a large number of images taken under controlled conditions. We circumvent these problems by estimating the ABRDF field from a few 2D images (which unlike the BRDF field, also takes into account the context of a point).

In this paper we present a novel method for approximating the facial ABRDF using higher-order (3^{rd} and 5^{th}) anti-symmetric Cartesian tensors. Unlike the Lambertian model, which is a 1^{st}-order tensor, higher-order Cartesian tensors can approximate the complex geometry of spherical functions with several lobes and therefore can handle shadows and better approximate the specular components of the facial ABRDF. Furthermore, in order to avoid overfitting

*This research was in part funded by the University of Florida Alumni Fellowships to A. Barmpoutis and R. Kumar. US patent pending.

978-1-4244-2243-2/08/$25.00 ©2008 IEEE

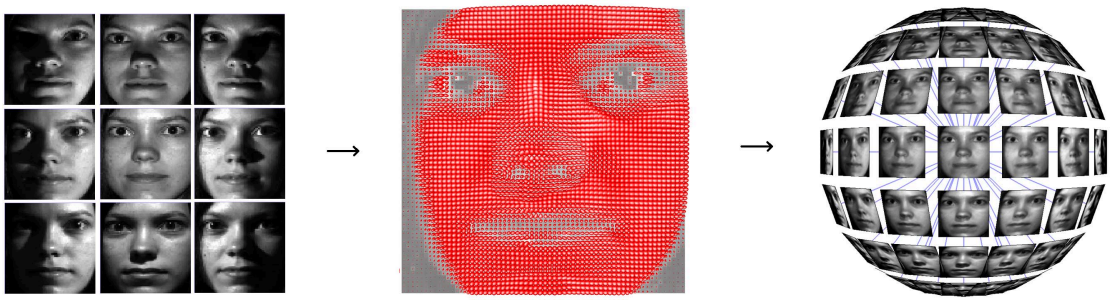

Figure 1. Illustration of our proposed anti-symmetric tensor spline model. Given a set of 9 images (left) associated with lighting directions, we estimate a cubic spline field (center) of 3^{rd}-order anti-symmetric tensors and then we employ it to relight the subject using any random lighting direction (right). Our model can produce realistic images, handling the specularities commonly seen in faces and casting shadows.

problems due to the small number of input images, we use a bi-cubic B-spline basis as the smoothing/weighting function of our anti-symmetric tensor-fields. We call this framework "Anti-symmetric tensor spline" (see Fig. 1). Given only a few input images (as few as 9) with different known lighting directions, we approximate the underlying facial ABRDF by an anti-symmetric tensor spline, and then using it we synthesize images under novel illumination (relighting).

In order to evaluate quantitatively the capability of our method in approximating facial ABRDFs, we also present a novel method for approximating the underlying true ABRDF using a continuous mixture of single-lobed spherical functions. This continuous mixture model, admittedly less efficient than our anti-symmetric tensor spline (as it requires a larger number of input images compared to tensor splines) can successfully approximate spherical functions with arbitrarily large number of lobes. In our experimental results we use the continuous mixture model as a validating benchmark to show that the proposed tensor spline model can approximate the facial ABRDF field to sufficient accuracy.

2. Anti-Symmetric Tensor Splines

In this section we introduce anti-symmetric tensor splines as splines of tensor-valued functions.

2.1. Spherical functions modeled as Tensors

A spherical function can be approximated by a n^{th}-order Cartesian tensor, which can be expressed in the form:

$$T(\mathbf{v}) = \sum_{k+l+m=n} T_{k,l,m}(v_1)^k(v_2)^l(v_3)^m \qquad (1)$$

where $\mathbf{v} = [v_1\ v_2\ v_3]^T$ is a unit vector and $T_{k,l,m}$ are the real-valued tensor coefficients. It should be noted that the spherical functions modeled by Eq. 1 are symmetric ($T(\mathbf{v}) = T(-\mathbf{v})$) for even orders, and anti-symmetric ($T(\mathbf{v}) = -T(-\mathbf{v})$) for odd orders. As a special case of Eq. 1 the 1^{st}-order tensors take the form $T(\mathbf{v}) = \mathbf{T} \cdot \mathbf{v}$, where $\mathbf{T} = [T_{1,0,0}\ T_{0,1,0}\ T_{0,0,1}]$ and the 2^{nd}-order tensors take the form $T(\mathbf{v}) = \mathbf{v}^T\mathbf{T}\mathbf{v}$, where $\mathbf{T}$ is a 3×3 matrix. It should be noted that in the case of 3^{rd}-order anti-symmetric tensors there are 10 unique coefficients $T_{k,l,m}$ in Eq. 1, while in the case of 5^{th}-order anti-symmetric tensors there are 21.

The ability of a Cartesian tensor to approximate the complex geometry of a spherical function with multiple lobes increases with its order. However, higher-order tensors can be perceived to be more sensitive to noise, simply by virtue of their ability to model high frequency detail. Since it is impossible to discriminate between high frequency detail in the data and high frequency noise in the data, it is reasonable to say that the high order tensors possess higher noise sensitivity. Thus we need to strike a balance between the approximation and the noise sensitivity of the fitted tensor.

2.2. Tensor Splines

In this subsection we define tensor splines by combining a) the Cartesian tensor basis within a single pixel (presented in Sec. 2.1) and b) the well known B-Spline basis across the image lattice [7]. Tensor splines were introduced first by Barmpoutis et al. in [1]. For simplicity, we will fix here the degree of a spline to 3 (cubic spline), since this degree of continuity is commonly used in literature.

We define a tensor spline as a B-spline on multilinear functions of any order in general. In a tensor spline, the multilinear functions (anti-symmetric tensors in our case) are weighted by the B-spline basis $N_{i,k+1}$, where

$$N_{i,1} = \begin{cases} 1 & \text{if } t_i \leq t < t_{i+1} \\ 0 & \text{otherwise} \end{cases} \qquad (2)$$

and

$$N_{i,k}(t) = N_{i,k-1}(t)\frac{t - t_i}{t_{i+k-1} - t_i} + N_{i+1,k-1}(t)\frac{t_{i+k} - t}{t_{i+k} - t_{i+1}} \qquad (3)$$

The $N_{i,k+1}(t)$ functions are polynomials of degree k, associated with n+k+2 monotonically increasing numbers

called "knots" $(t_{-k}, t_{-k+1}, ..., t_{n+1})$.

By using the above, the equation of a bi-cubic (k=3) tensor spline is given by:

$$S(\mathbf{t}, \mathbf{v}) = \sum_{i,j} N_{i,4}(t_x) N_{j,4}(t_y) T_{i,j}(\mathbf{v}) \tag{4}$$

where $\mathbf{t} = [t_x \ t_y]$, $\mathbf{v} = [v_1 \ v_2 \ v_3]^T$ is a unit vector, and $T_{i,j}(\mathbf{v})$ is given by Eq. 1. It should be noted that in Eq. 4 there is a field of control tensors $T_{i,j}(\mathbf{v})$, instead of the control points used in a regular B-spline [7].

In the next subsection we employ bi-cubic tensor splines for approximating the ABRDF field of a human face given a set of fixed-pose images under different known lighting directions.

2.3. Apparent BRDF approximation by Tensor Splines

The BRDF of a Lambertian surface is given by $B(\mathbf{v}) = \alpha(\mathbf{n} \cdot \mathbf{v})$, where the negative values are set to zero and $\mathbf{v}$ is the light-source direction, $\mathbf{n}$ is the normal vector at a particular point of the surface and α is a constant. It is immediate that the Lambertian model is in the form of a 1^{st}-order tensor (Eq. 1 for n=1) with $T_{1,0,0} = \alpha n_x$, $T_{0,1,0} = \alpha n_y$ and $T_{0,0,1} = \alpha n_z$. As a 1^{st}-order tensor, the Lambertian model is anti-symmetric and has a single peak.

Human faces however are not exactly Lambertian since specularity can be observed in certain regions (e.g. nose, forehead). Moreover, the non-convex shapes on the face (lips, nose) can create cast shadows. The shadows and specularities of the human face are indicative of a multi-lobed ABRDF. Therefore, in these cases the ABRDF cannot be modeled successfully by a 1^{st}-order tensor and hence higher-order anti-symmetric tensors should be employed instead.

Our problem can be defined as follows. Given a set of N face images of a given human subject with fixed pose, I_n, $n = 1 \dots N$ with associated lighting directions $\mathbf{v}_n$, we want to estimate the ABRDF field of the face using a bi-cubic tensor spline. The fitting of the tensor spline to the given data can be done by minimizing the following energy

$$E = \sum_{n=1}^{N} \sum_{t_x, t_y} \left(\sum_{i,j} N_{i,4}(t_x) N_{j,4}(t_y) T_{i,j}(\mathbf{v}_n) - I_n(t_x, t_y) \right)^2 \tag{5}$$

where t_x, t_y run through the lattice of the given images. The minimization of Eq. 5 is done with respect to the unknown tensor coefficients $T_{i,j,k,l,m}$ that correspond to the control tensor $T_{i,j}(\mathbf{v}_n)$. In our experiments we used an uniform grid of knots $1, 2, 3 \dots$ in both lattice coordinates. There were $(M+2) \times (M+2)$ control tensors, where $M \times M$ is the lattice size of each given image. Under this configuration, in the case of 3^{rd}-order anti-symmetric tensors, there are 10 unique coefficients for each control tensor; therefore the number of unknowns in Eq. 5 is equal to $10(M+2)^2$. In the case of 5^{th}-order anti-symmetric tensors the number of unknowns is $21(M+2)^2$. Although, given 9 input images the number of known samples is $9M^2$, there is no overfitting issue (at least in the proposed case of 3^{rd}-order tensors) due to the B-spline regularization. From Eq. 5 we can analytically compute the derivatives $dE/dT_{i,j,k,l,m}$ and thus any gradient-based functional minimization method can be used. To evaluate the performance of tensor splines, in the next section we define a validating model using continuous mixture of single-lobed functions.

3. Continuous Mixture of single-lobed functions

A natural question to ask is whether the tensor spline model is capable of approximating ABRDFs on human faces. In order to give a quantitative answer to this question we need to compare tensor splines with a more general model, which can, in theory, approximate spherical functions with arbitrarily many lobes. In this section we define such a general model for approximating spherical functions using a continuous mixture of single-lobed spherical functions. The framework of continuous mixture of functions was introduced by Jian et al. in [14].

There are various spherical functions with a single lobe that can be used in a continuous mixture but we pick one which leads to an analytic solution, given by $S(\mathbf{v}) = e^{-\mathbf{u}\cdot\mathbf{v}} - 1$, where $\mathbf{u}$ and $\mathbf{v}$ are unit vectors. Note that this function has the following two desirable properties: a) it has a single peak, and b) $S(\mathbf{v}) = 0$ for all $\mathbf{v}$ such that $\mathbf{v} \cdot \mathbf{u} = 0$ (because if the surface normal and illumination direction are perpendicular we expect zero intensity). These properties are also valid for the Lambertian model.

With this definition of the single-lobed function any spherical function can be written as a continuous mixture of such functions. So the ABRDF, a spherical function, can be modeled as a continuous mixture of functions $S(\mathbf{v})$ as follows

$$B(\mathbf{v}) = \int_{S_2} f(\mathbf{u})(e^{-\mathbf{u}\cdot\mathbf{v}} - 1) d\mathbf{u} \tag{6}$$

where the integration is over the set of all unit vectors $\mathbf{u}$ (i.e. unit sphere) and $f(\mathbf{u})$ is a distribution on orientations. As von Mises-Fisher is the analog of the Gaussian distribution on S_2, we pick it as the mixing density. The von Mises-Fisher distribution is given by

$$f(\mathbf{u}|\kappa, \mu) = \frac{\kappa e^{\kappa \mu \cdot \mathbf{u}}}{4\pi sinh(\kappa)} \tag{7}$$

where μ is a unit vector defining the orientation and κ is a scalar governing the concentration of the distribution.

Here we make the *important* observation that by substituting Eq. 7 into Eq. 6 we obtain an integral which is the Laplace transform of the von Mises-Fisher distribution, which we have analytically computed to be

$$B(\mathbf{v}) = \frac{\kappa sinh(\|\kappa\mu - \mathbf{v}\|)}{sinh(\kappa)\|\kappa\mu - \mathbf{v}\|} - 1. \quad (8)$$

However the single von Mises-Fisher distribution model cannot approximate angular distributions with several peaks, like the human face ABRDFs. Therefore, we propose to use a finite mixture of von Mises-Fisher distributions, which leads to an alternate definition of Eq. 7 as $\tilde{f}(\mathbf{u}) = \sum_i w_i f(\mathbf{u}|\kappa, \mu_i)$, where w_i are the mixture weights. In our implementation we used a dense sampling (642 directions) of the unit sphere obtained by the 4^{th}-order tessellation of the icosahedron. Using this mixture of von Mises-Fisher distributions we obtain the following expression for the ABRDF

$$B(\mathbf{v}) = \sum_i w_i \left(\frac{\kappa sinh(\|\kappa\mu_i - \mathbf{v}\|)}{sinh(\kappa)\|\kappa\mu_i - \mathbf{v}\|} - 1 \right) \quad (9)$$

We must emphasize that although $\tilde{f}(\mathbf{u})$ has the form of a discrete mixture, the approximating function $B(\mathbf{v})$ is still a continuous mixture of single-lobed functions expressed by Eq. 6.

Given a set of N face images I_n, $n = 1 \dots N$, of a human subject with the same fixed pose, associated with lighting directions $\mathbf{v}_n$, we can set up a $N \times 642$ matrix $\mathbf{A}_{n,i}$ by evaluating Eq. 8 for every $\mathbf{v}_n$ and μ_i. Then for each pixel we can estimate the unknown weights of Eq. 9, by solving the overdetermined system $\mathbf{AW} = \mathbf{B}$, where $\mathbf{B}$ is a N-dimensional vector that consists of the intensities of a fixed pixel in the N given images, and $\mathbf{W}$ is the vector of the unknown weights. This system can be solved efficiently to obtain a sparse solution by the non-negative least square minimization algorithm developed in [15].

For the experiments presented in Sec. 4 we use the model presented in this section as a benchmark for evaluating quantitatively the ability of the proposed anti-symmetric tensor splines in approximating the ABRDF of human faces.

4. Experimental Results

4.1. Face Image Synthesis

All the experiments in this section used the Extended Yale B database [17], which has 64 different images per subject under known illumination directions. After the training was performed using only 9 images per subject according to the method described in Sec. 2.3, we synthesized 64 facial images per subject by evaluating Eq. 4 for the 64 lighting directions provided in the database.

Figure 2. Example of facial image relighting. The images were synthesized by evaluating the anti-symmetric tensor spline for different extreme lighting directions.

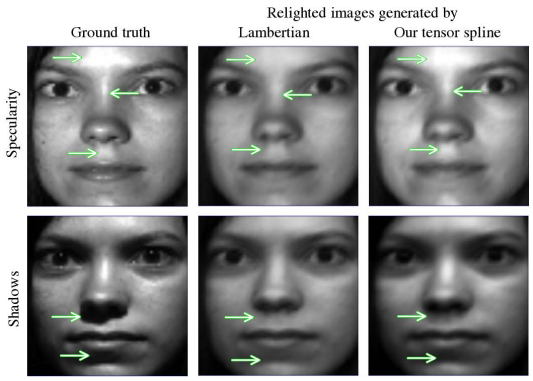

Figure 3. Demonstration of the ability of our method to handle cast shadows and specularities. First column: ground truth images, second column synthesized images using Lambertian model, last column synthesized images using our 3^{rd}-order anti-symmetric tensor spline model.

Figure 2 presents the synthesized images under several different lighting directions for a randomly selected subject. The images demonstrate that our proposed model approximated well the underlying ABRDF, producing realistic images. The 9 input images used here are shown in Fig.1.

In Fig. 3 we show some examples of the synthesized images using the Lambertian model and our tensor spline model for visual comparison. The first column shows the ground truth image from the extended Yale B dataset. Note that the ground truth images presented in this figure were not part of the training set used for the synthesis of the images presented in the second and third columns of the figure. By visual comparison we conclude that the 3^{rd}-order tensorial model can accommodate cast shadows and approximate well the specular components of the ABRDFs. In contrast, specularity and shadows are missing from the images synthesized under the Lambertian model which demonstrates the invalidity of the Lambertian assumption.

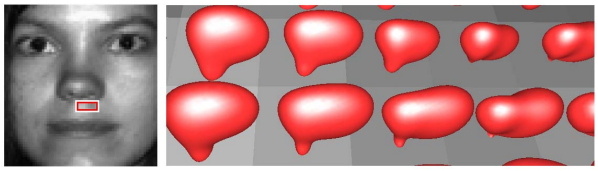

Figure 4. Example of the approximated ABRDFs plotted as spherical functions in a region of interest shown in a rectangle on the left image.

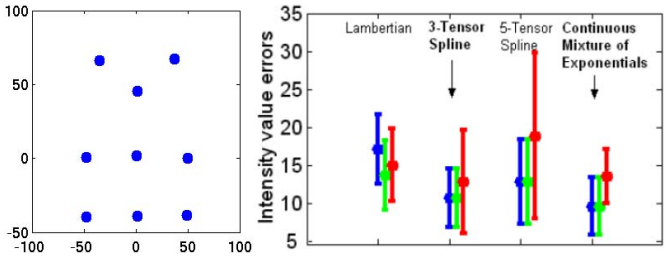

Figure 5. Left: The 9 input lighting directions we used (shown in the azimuth-elevation plane). Right: Intensity value error comparison of several models. The blue color represents the standard 1^{st} and 2^{nd} category which contain lighting directions forming angle ϕ with the frontal direction smaller than 25^o, the green color represents the 3^{rd} category with $25^o < \phi < 50^o$ and the red color represents the 4^{th} category with $50^o < \phi < 70^o$.

Figure 4 shows the approximated ABRDFs plotted as spherical functions in a region of interest that has specularities and shadows. The shapes of the plotted functions contain up to three lobes and show complexities that cannot be approximated under the Lambertian assumption.

Finally in order to evaluate the ability of our model to approximate facial ABRDFs, we employed the continuous mixture of single-lobed functions (proposed in Sec. 3) to approximate the underlying ABRDF by using all 64 given images as the training set. This model, although less efficient (since it requires a much larger training set of 64 images) than our anti-symmetric tensor spline model (which uses only 9 images), can approximate spherical functions with a very complex structure characterized by a large number of lobes. In contrast, our 3^{rd}-order anti-symmetric tensor spline model can approximate functions whose shape complexity consists of at most three lobes. By comparing the performance of the continuous mixture of exponential functions with that of our anti-symmetric tensor spline, both presented in Fig. 5(right), we conclude that they yield similar intensity values. This quantitatively demonstrates that inspite of the limitations of the 3^{rd}-order anti-symmetric tensor spline model, we can still capture and approximate the shape of the underlying facial ABRDFs.

4.2. Application of our method to Face Recognition

Our proposed method of anti-symmetric tensor splines can also be used in face recognition applications. Given a set of fixed-pose images under different known illuminating directions for N subjects (human faces), the problem of face recognition is to assign to a new test image, a label corresponding to one of the N given subjects. We assume that the new image is provided in the same pose as the N known subjects, albeit under an unknown illuminating direction.

By employing our method proposed in Sec. 2.3 we can approximate the apparent BRDF of each subject by an anti-symmetric tensor spline. Thus, by using our method we can convert the given dataset of facial images into a dataset of anti-symmetric tensor splines. Then, given an unknown test image I, it is classified by minimizing the following function:

$$\min_{n\in[1,\dots N],\mathbf{v}\in S_2} \sum_{\mathbf{t}} \left(S_n(\mathbf{t},\mathbf{v}) - I(\mathbf{t})\right)^2 \qquad (10)$$

where $S_n(\mathbf{t},\mathbf{v})$ is the anti-symmetric tensor spline of subject n given by Eq. 4, $\mathbf{v}$ is a unit vector and $\mathbf{t}$ is the 2-dimensional image lattice index. By minimizing Eq. 10 we simultaneously estimate a) the label n of the unknown test image and b) the unknown lighting direction $\mathbf{v}$ of the test image. The minimization of Eq. 10 can be performed by any gradient-based functional minimization algorithm. We can parameterize the unit vector $\mathbf{v}$ by using polar coordinates and then compute for each subject the gradient of Eq. 10 with respect to the azimuth θ and elevation ϕ angles.

Table 1 shows the percentages of recognition errors for the standard categories of the test image lighting directions (described in Fig. 5). The table also contains recognition percentage errors obtained on the same dataset using other existing methods such as Correlation [6], Eigenfaces [12], Linear subspace [4], Illumination cones [11] and 9 points of lighting (9PL) [17]. The errors for the first five techniques were taken from the table presented in [11]. A comparison of the error rates show that our proposed model performs significantly better than the Correlation, Eigenfaces, Linear Subspace and Illumination cones-attached methods and slightly better than the 9PL method. Illumination cones-cast method, the only technique which performs slightly better than our model, suffers from inefficiencies inherent in extracting 3D information using photometric stereo, while our technique does not involve any such cubersome step.

In our experiments, we used a training set that corresponded to the lighting direction configuration shown in Fig. 5(left) since this samples well the lighting direction space and yielded better ABRDF approximations. For other lighting configurations, which do not sample the azimuth-elevation space well and therefore do not represent the underlying data well, there was a slight increase (2-5%) in the percentage errors for the 4^{th} category. This result is ex-

Method	N samples	$1^{st}\&2^{nd}$	3^{rd}	4^{th}
Correlation [6]	4	0.0	23.3	73.6
Eigenfaces [12]	6	0.0	25.8	75.7
Linear subspace [4]	7	0.0	0.0	15.0
Cones-attached [11]	7	0.0	0.0	8.6
Cones-cast [11]	7	0.0	0.0	0.0
9PL [17]	9	0.0	0.0	2.8
Our method	9	0.0	0.0	1.6

Table 1. Face recognition percentage errors for several existing methods for the standard 4 categories of the test set. The second column reports the minimum number of required training images.

pected, since in any application that involves sampling, the performance is significantly better when the samples represent the data well.

5. Discussion

By approximating the local apparent BRDF of a human face using the model of continuous mixture of a single-lobed function presented in Sec.3, we show that in general the number of lobes in a facial apparent BRDF is at most 3. We also show that such a complex spherical function can be efficiently approximated using a 3^{rd}-order anti-symmetric tensor spline. The continuous mixture model requires a large number of training images for representing the apparent BRDF effectively, and therefore performs worse (in terms of time complexity) than our proposed anti-symmetric tensor spline model which uses only 9 images.

Another advantage of the tensor spline model is that it models the apparent BRDF function by using only 10 scalar coefficients. Noting that the extended Yale B dataset contains 64 images for each subject, our proposed method "compresses" all the given information into 10 images corresponding to the 3^{rd}-order tensor coefficients.

Finally, we should note that a limitation of our method is that it requires the lighting directions of the training images to be known. However this limitation can be overcome if we create a generic tensor spline face by taking, for example, the average of the tensor splines that approximate the subjects in the extended Yale B database. We can then estimate the unknown lighting direction of a new image by following a functional minimization method similar to that described by Eq. 10 in Sec. 4.2. By incorporating this "lighting direction recovery" step, our method can work with any set of fixed-pose facial images with unknown lighting directions.

References

[1] A. Barmpoutis, et al. Tensor splines for interpolation and approximation of DT-MRI with applications to segmentation of isolated rat hippocampi. *TMI*, 26(11):1537–1546, 2007.

[2] R. Basri and D. Jacobs. Lambertian reflectance and linear subspaces. *PAMI*, 25(2):218–233, 2003.

[3] A.U. Batur and M. Hayes. Linear subspaces for illumination robust face recognition. *CVPR 2001*, 2:296–301, 2001.

[4] P. Belhumeur, D. Kriegman, and A. Yuille. The bas-relief ambiguity. *CVPR 1997*, 1040–1046, 1997.

[5] G. Borshukov and J. P. Lewis. Realistic human face rendering for "the matrix reloaded". In *ACM SIGGRAPH 2003 Sketches & Applications*, pages 1–1, 2003.

[6] T. Brunelli, R.; Poggio. Face recognition: features versus templates. *PAMI*, 15(10):1042–1052, Oct 1993.

[7] C. de Boor. On calculating with b-splines. *J. Approx. Theory*, 6:50–62, 1972.

[8] P. Debevec, et al. Acquiring the reflectance field of a human face. In *SIGGRAPH*, pages 145–156, 2000.

[9] S. C. Foo. A gonioreflectometer for measuring the bidirectional reflectance of material for use in illumination computation. *Master's thesis, Cornell University, Ithaca*, 1997.

[10] M. Fuchs, et al. Reflectance from images: A model-based approach for human faces. *TVCG*, 11(3):296–305, 2005.

[11] A. S. Georghiades et al. From few to many: Illumination cone models for face recognition under variable lighting and pose. *PAMI*, 23(6):643–660, 2001.

[12] P. Hallinan. A low-dimensional representation of human faces for arbitrary lighting conditions. *CVPR*, pages 995–999, 21-23 Jun 1994.

[13] B. K. P. Horn. *Robot Vision*. McGraw Hill: New York.

[14] B. Jian, et al. Multi-fiber reconstruction from Diffusion MRI using Mixture of Wisharts. *IPMI*, 384–395, 2007.

[15] C. Lawson and R. J. Hanson. *Solving Least squares problems.* Prentice-Hall, Englewood Cliffs, 1974.

[16] J. Lee, et al. A bilinear illumination model for robust face recognition. In *ICCV*, pages 1177–1184, 2005.

[17] K. Lee, et al. Acquiring linear subspaces for face recognition under variable lighting. *PAMI*, 27(5):684–698, 2005.

[18] W. Matusik, et al. A data-driven reflectance model. In *SIGGRAPH*, pages 759–769, 2003.

[19] P. J. Phillips, H. Moon, S. A. Rizvi, and P. J. Rauss. The FERET evaluation methodology for face-recognition algorithms. *PAMI*, 22(10):1090–1104, 2000.

[20] Y. Sato, et al. Object shape and reflectance modeling from observation. *SIGGRAPH*, 31:379–388, 1997.

[21] A. Shashua and T. Riklin-Raviv. The quotient image: Class-based re-rendering and recognition with varying illuminations. *PAMI*, 23(2):129–139, 2001.

[22] T. Sim, et al. The CMU pose, illumination, and expression database. *Automatic Face and Gesture Recognition*, 2002.

[23] Z. Wen, Z. Liu, and T. S. Huang. Face relighting with radiance environment map. In *CVPR*, pages 158–65, 2003.

[24] T. Weyrich, et al. Analysis of human faces using a measurement-based skin reflectance model. In *SIGGRAPH*, pages 1013–1024, 2006.

[25] L. Zhang et al. Face recognition under variable lighting using harmonic image exemplars. In *CVPR*, pages 19–25, 2003.

[26] L. Zhang, et al. Face synthesis and recognition from a single image under arbitrary unknown lighting using a SH basis morphable model. In *CVPR*, pages 209–216, 2005.